NEW ALGORITHM FOR SUB-PIXEL BOUNDARY MAPPING

Yong Ge[a], Sanping Li[a,b], Deyu Li[b]

[a] State Key Laboratory of Resources and Environmental Information System, Institute of Geographic Sciences & Natural Resources Research, Chinese Academy of Sciences, Beijing 100101, China - gey@lreis.ac.cn
[b] School of Computer and Information Technology, Shanxi University, Taiyuan, 030006

KEY WORDS: Mixed Pixel, Endmember, Spatial Pattern, Sub-Pixel Boundary Mapping

ABSTRACT:

Remotely sensed images often contain a combination of both pure and mixed pixels. Analysis and classification of remotely sensed imagery used to provide information on the spatial pattern of land cover feature suffer from the problem of class mixing within pixels. Therefore, how to get spatial pattern and boundaries information of endmembers in sub-pixel scale has been receiving increasing attention over recent years. A new algorithm for sub-pixel boundary mapping has been proposed in this paper to map the spatial arrangement of land cover targets within pixels. The validity of the technique is demonstrated by applying it to controlled simulated artificial images.

1. INTRODUCTION

The existence of mixed pixel, consisting of different features smaller than the resolution of the sensor, is one of the main sources affecting the accuracy of classification. Soft classification techniques can estimate the class composition of image pixels. Their outputs, however, provide no indication of spatial distribution of such classes within a pixel. Mapping subpixel scale land cover features has been developed over recent years. Atkinson (1997a) started this issue, based on the assumption of spatial dependence within and between pixels, by determining where the relative proportions of each class occur within each pixel. Later, Aplin et al. (1999 and 2001) proposed a set of techniques on a per-parcel (herein termed per-field) basis by integrating fine spatial resolution simulated satellite sensor imagery with digital vector data to classify land cover. Tatem et al. (2000, 2001a, 2001b, 2002, 2003) proposed an algorithm to predict the spatial pattern of objects smaller than the ground resolution of the sensor by incorporating prior information on the typical spatial arrangement of the particular land cover types into the energy function of Hopfield neural network as a semivariance constraint. Mertens et al. (2003) proposed a method of combining genetic algorithm with the assumption of spatial dependence to assign a location to every subpixel by evaluating all possible configurations of the subpixels inside a pixel according to the parameter, the neighbouring value. These techniques enable the utilization of providing spatial distribution of classes within pixels. However, high resolution images (Atkinson, 1997b), prior information (Tatem et al., 2002, 2003) or vector data (Aplin et al., 1999 and 2001) as auxiliary data need to be collected prior to implementing these methods. Consequently, some of them were time-consuming. For instance, the running time of the approach proposed by Tatem et al. (2003) used on the task of mapping from real Landsat TM agriculture imagery to derive accurate estimates of land cover was approximately 210 minutes and 510 minutes on a PII-350 computer respectively. Therefore, the technique presented in this paper attempts to overcome these problems and to present a novel and effective solution to mapping the spatial distribution classes within pixels. It utilizes the proportions of every endmember component within central pixel and its 8 neighboring pixels, which are from a soft classification assigning pixel fractions to the land cover classes corresponding to the represented area inside a pixel, to achieve the location of every endmember component within central pixel. The validity is demonstrated by applying it to a controlled simulated artificial image.

2. MAPPING BOUNDARIES OF ENDMEMBERS WITHIN MIXED PIXEL

Assume that a mixed pixel P_C, depicted in Figure 1, contains two endmember components A and B. The area proportion vector of endmembers $\{a_C, b_C\}$ and that of neighboring pixel P_i denoted $\{a_i, b_i\}$ ($i = 0, 1, \cdots, 7$) can be estimated by soft classification techniques implemented some commercial software for remote sensing image processing such as RSI ENVI, and ERDAS IMAGINE, etc.
In Figure 1, P_C composes of four vertexes L, C, F and I, respectively. The whole boundary of P_C is divided equally into eight parts in length. The divided line segments are AB, BCD, DE, EFG, GH, HIJ, JK and KLA, respectively, where $AB = 2BC$, $LC = 2AB$, etc. Each of surrounding pixels corresponds to a one-eighth line segment. For example, P_0 corresponds to AB and P_1 corresponds to BCD. Similarly, the rest surrounding pixels correspond to the rest line segments successively. MON and POQ described in Figure 1, are two line segments intersecting perpendicularly at the center O and are equal in length which is equal to AB. The basic idea of this method, based on the assumption of spatial dependence within and between pixels, is to determine the boundary of endmember A (B) within P_C by use of the values of a_C (b_C), a_i (b_i), eight line segments and MON and POQ. In next subsection, we will explain how it works step by step. Without loss of generality, we discuss the cases: AB, MON and POQ.

(A) Determining the length of V_{AB} in AB

Defined a line segment V_{AB} in AB, its length and location in AB is used to account for the contribution of the endmember A of neighboring pixels P_0, P_1, P_7 to the boundary of the endmember A within P_C. The length of V_{AB} is less than or equal to the length of AB. Consequently, AB is also divided equally into eight parts, and the dividing points are denoted as T_3, T_2, T_1, T, T_4, T_5, T_6, as shown in Figure 2. There is three situations below to determine the length of V_{AB}: (I) If $a_0 = 1$, then V_{AB} equals to the length of AB. (II) If $a_0 = 0$, then $V_{AB} = 0$. (III) If $0 < a_0 < 1$, then $V_{AB} = \frac{[a_0 / 0.125]}{8} \cdot |AB|$, where $[x]$ is the rounded number of real number x.

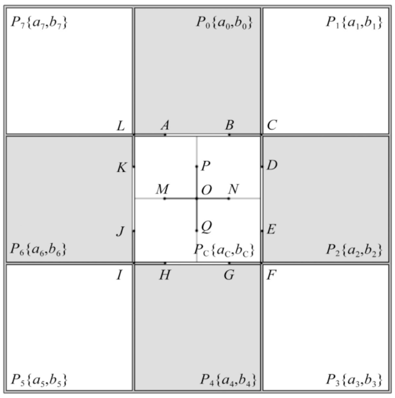

Figure 1. Central pixel P_C, neighboring pixel P_i and the inside and boundary of the pixel P_C

(B) Determining the location of V_{AB} in AB

After obtaining the length value V_{AB} in AB, we then determine the location of V_{AB} in AB. The determining process includes two steps.

Step 1: Initial position $V_{AB}^{(0)}$.

Starting with the mid-point T of the line segment AB, one can take dividing points from AB on the both sides of T till the length of all divided parts equals to V_{AB}. As illustrations in figure 2, T_1T_4 was marked as 0.25 on the line segment AB, i.e., when $a_0 = 0.25$, $V_{AB}^{(0)} = |T_1T_4|$. Similarly, if $a_0 = 0.50$, $V_{AB}^{(0)} = |T_2T_5|$ and if $a_0 = 0.75$, $V_{AB}^{(0)} = |T_3T_6|$.

Step 2: Calculating position offset Δ_{AB}.

If the numbers of dividing points on the both sides of T are not equal, an offset arises, that is we need to adjust the position of V_{AB} according to the comparison of values of a_1 and a_7. For instance, when $a_0 = 0.375$, $V_{AB}^{(0)} = |T_1T_5|$ if a_1 is greater than a_7, otherwise $V_{AB}^{(0)} = |T_2T_4|$. The offset can be calculated below

$$\Delta_{AB} = \begin{cases} [|a_1 - a_7| \cdot (1 - a_0)/0.25], & 0 < a_0 \le 1 \\ 0, & a_0 = 0 \end{cases} \quad (1)$$

In equation (1), the unit of offset Δ_{AB} is $\frac{|AB|}{8}$, which refers to a one-eighth length of the line segment AB. Adding the offset Δ_{AB} to $V_{AB}^{(0)}$, the final position of V_{AB} can be obtained.

(C) Determining the lengths and locations of V_{MON} in MON and V_{POQ} in POQ

The point O is the center of pixel P_C. The line segments MON and POQ are perpendicular and their lengths are equal to the half of the edge length of pixel P_C, and $OP = OQ$, $OM = ON$. Dividing the line segments PQ and MN into eight equal parts respectively, one can get the equally divided points which are V_3, V_2, V_1, O, V_4, V_5, V_6, and U_3, U_2, U_1, O, U_4, U_5, U_6 described in Figure 2. In horizontal direction, the length and location of V_{MON} can be determined by use of a_C, a_2 and a_6. While in the vertical direction, the length and location of V_{POQ} can be determined by use of a_C, a_0 and a_4.

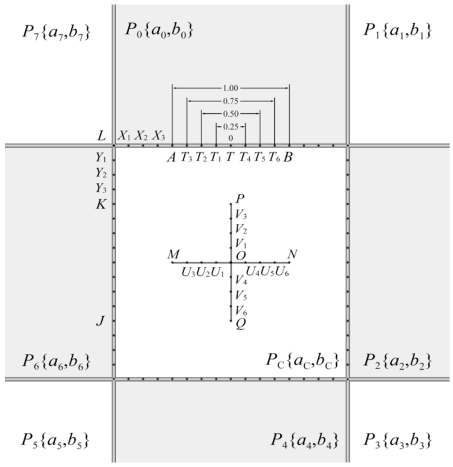

Figure 2. The neighboring pixels and center pixel in boundary line segments of P_C with area pattern

(D) Determining the boundary of endmember A in P_C

After achieving the length and location of line segments in four sides of P_C, MON and POQ, one connects the vertexes identified by these line segments to form a polygon. The polygon is the boundary of endmember A within P_C. Repeatedly, we can simulate the spatial distribution of the background endmember B within the pixel P_C using the values of b_i and b_C.

3. EMPIRICAL ANALYSIS OF ARTIFICIAL IMAGES

As shown in Figure 3(a), curve $Z_1Z_2Z_3$ was the real boundary of the endmember A and the background member B between the central pixel P_C and its neighbouring pixel P_i. The area of the endmember component A and the background component B in each pixel is: $P_C\{0.60, 0.40\}$, $P_0\{0.15, 0.85\}$, $P_1\{0.0, 1.0\}$, $P_2\{0.0, 1.0\}$, $P_3\{0.11, 0.89\}$, $P_4\{0.94, 0.06\}$, $P_5\{1.0, 0.0\}$, $P_6\{1.0, 0.0\}$ $P_7\{0.65, 0.35\}$, respectively.

Step 1: First computing the length and location of neighboring pixel P_0 on AB which is the boundary line of P_C. Given that the area which is belong to A of P_0, P_1, P_7 separately is $a_0 = 0.15$, $a_1 = 0.0$, $a_7 = 0.65$, so the length of the AB which is the boundary line of A on P_C is:

$$V_{AB} = \frac{\left[0.15/0.125\right]}{8} \cdot |AB| = \frac{\left[1.2\right]}{8} \cdot |AB| = \frac{1}{8} \cdot |AB| \tag{2}$$

The initial position of V_{AB} is $V_{AB}^{(0)} = |TT_1|$. The displacement of position is:

$$\Delta_{AB} = \left[\, |0.65 - 0.0| \times (1 - 0.15)/0.25 \,\right] = \left[2.21\right] = 2 \tag{3}$$

The direction of the displacement is the side of the pixel P_7, then the final position of V_{AB} is $V_{AB}^{(1)} = |T_2T_3|$.

Step 2: calculating the length and position of P_7 on the boundary ALK of P_C. Given the area which is belong to A of P_0, P_7, P_6 separately is $a_0 = 0.15$, $a_7 = 0.65$, $a_6 = 1.0$, then the length of ALK which is the boundary line of the endmember A on P_C is:

$$V_{ALK} = \frac{\left[0.65/0.125\right]}{8} \cdot |ALK| = \frac{\left[5.2\right]}{8} \cdot |ALK| = \frac{5}{8} \cdot |ALK| \tag{4}$$

the initial position of V_{ALK} is $V_{ALK}^{(0)} = |Y_3LX_2|$. The displacement of position is:

$$\Delta_{ALK} = \left[\, |1.0 - 0.15| \times (1 - 0.65)/0.25 \,\right] = \left[1.19\right] = 1 \tag{5}$$

the direction of the displacement is the side of the pixel P_6,then the final position of V_{ALK} is $V_{ALK}^{(1)} = |KLX_1|$.

Step 3: Reckoning the length and position of the central pixel P_C at the cross line of intersection MON, POQ. Suppose $a_C = 0.60$, $a_6 = 1.0$, $a_2 = 0.0$, then the length of P_C on the line segment MON is:

$$V_{MON} = \frac{\left[0.60/0.125\right]}{8} \cdot |MON| = \frac{\left[4.8\right]}{8} \cdot |MON| = \frac{5}{8} \cdot |MON| \tag{6}$$

The initial position of V_{MON} is: $V_{MON}^{(0)} = |U_3OU_5|$. The displacement of position is:

$$\Delta_{MON} = \left[\, |1.0 - 0.0| \times (1 - 0.60)/0.25 \,\right] = \left[1.0\right] = 1 \tag{7}$$

The direction of the displacement is the side of the pixel P_6,then the final position of V_{MON} is $V_{MON}^{(1)} = |MOU_4|$.

For the same principle, if $a_C = 0.60$, $a_0 = 0.15$, $a_4 = 0.94$, then we can calculate the length of P_C on the line segment POQ:

$$V_{POQ} = \frac{\left[0.60/0.125\right]}{8} \cdot |POQ| = \frac{\left[4.8\right]}{8} \cdot |POQ| = \frac{5}{8} \cdot |POQ| \tag{8}$$

the initial position of V_{POQ} is $V_{POQ}^{(0)} = |V_2OV_6|$.The displacement of position is:

$$\Delta_{POQ} = \left[\, |0.15 - 0.94| \times (1 - 0.60)/0.25 \,\right] = \left[1.264\right] = 1 \tag{9}$$

The direction of the displacement is the side of the pixel P_4,then the final position of V_{POQ} is $V_{POQ}^{(1)} = |V_1OQ|$.

Step 4: Using the pixel's internal geographical object boundary value rule iteratively, finally we can obtain the spatial distribution's simulated result of the endmember A's pixel P_C, as is shown in Figure 3(b). The pixel P_C's boundary and internal value of the neighboring pixel P_i and central pixel P_C is shown as white line segment in Figure 3(b). The value of P_0 at the boundary of pixel P_C is T_3T_2,the value of P_1, P_2 is null, P_3's value is line segment G_1G,the value of P_4 is line segment HG, P_5's value is the curve HIJ, P_6's value is line segment JK, P_7's value is curve KLX_1.Pixel P_C's value at the horizontal direction is line segment MOU_4,at the vertical direction is line segment V_1OQ.The boundary point of the polygon which is determined by the value of these line segment is L, T_2, V_1, U_4, G_1, I, then we connect these point to form a polygon. An simulated distribution of endmember on pixel P_C can be obtained. P_C was divided into 16×16 units, the number of the gray unit is 146 ,which is the simulated distribution of endmember A on the pixel P_C. From the simulated distribution we can obtain the area of endmember A at the pixel P_C is $a_C^{'} = 146/256 = 0.57$, which is very similar to the real value of $a_C = 0.60$.

(a)

(b)

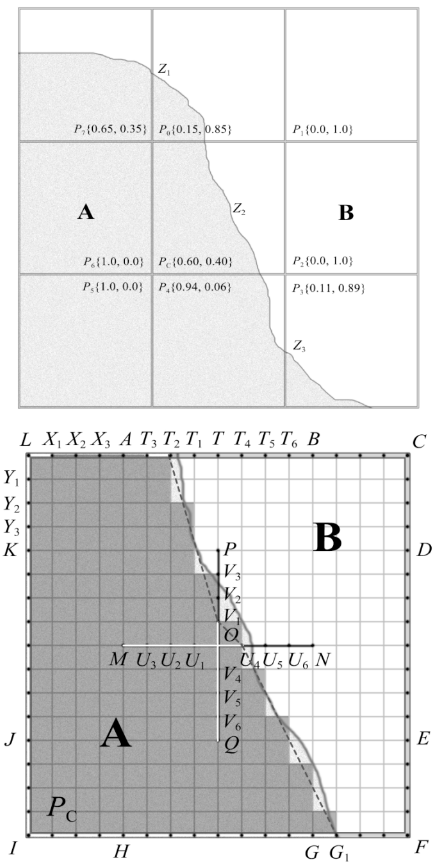

Figure 3. (a) Artificial image with two endmembers A and B; (b) Spatial distribution of endmember A within mixed pixel P_C by the technique proposed in this paper

4. CONCLUSION AND FUTURE WORKS

In this paper, a new algorithm for sub-pixel boundary mapping is proposed. Two simulated images were used for validating the method. It has been demonstrated that the technique is a simple, robust, and efficient tool for an existing super-resolution target identification technique.

Topics for further investigation include band patter and point pattern. Furthermore, we have only investigated the spatial distribution of endmember components in simply connected domain of area pattern. It will be essential to investigate the spatial distribution of endmember components in complex connected domain of area pattern.

REFERENCES

Aplin, P. & Atkinson, P.M., 2001. Sub-pixel land cover mapping for per-field classification. *International Journal of Remote Sensing*. Vol. 22, No. 14, pp. 2853-2858.

Aplin, P., Atkinson, P.M. & Curran, P.J., 1999. Fine spatial resolution simulated satellite sensor imagery for land cover mapping in the United Kingdom. *Remote Sensing of Environment*. Vol. 68, pp. 206-216.

Atkinson, P.M., 1997a. Mapping sub-pixel vector boundaries from remotely sensed images. In: Proceedings of GISRUK '96. University of Kent, Canterbury, UK, 29-41. In: Kemp Z. Edi: Innovations in GIS 4 [C], London: Taylor and Francis, 1997: 166-180.

Atkinson, P.M., Cutler, M.E.J. & Lewis, H., 1997b. Mapping sub-pixel proportional land cover with AVHRR imagery. *International Journal of Remote Sensing*, 18 (4), pp. 917-935.

Mertens, K.C., Verbeke, L.P.C., Ducheyne, E.I. & De Wulf, R.R., 2003. Using genetic algorithms in sub-pixel mapping. *International Journal of Remote Sensing,* Vol. 24, No. 21, pp. 4241-4247.

Tatem, A.J., Lewis, H.G., Atkinson, P.M. & Nixon, M.S., 2000. Land cover simulation and prediction at the sub-pixel scale using a Hopfield neural network. *Proceedings, 26th Annual Conference and Exhibition of the Remote Sensing Society*, Leicester, UK; 12-14 September 2000. The Remote Sensing Society, Nottingham.

Tatem, A.J., Lewis, H.G., Atkinson, P.M. & Nixon, M.S., 2001a. Super-resolution target identification from remotely sensed images using a Hopfield neural network. *IEEE Transactions on Geoscience and Remote Sensing*. Vol. 39, No. 4, pp. 781-796.

Tatem, A.J., Lewis, H.G., Atkinson, P.M. & Nixon, M.S., 2001b. Multiple class land cover mapping at the sub-pixel scale using a Hopfield neural network. *Journal of Applied Earth Observation and Geoinformation.* Vol. 3, No. 2, pp. 184-190.

Tatem, A.J., Lewis, H.G., Atkinson, P.M. & Nixon, M.S., 2002. Super-resolution land cover pattern prediction using a Hopfield neural network. *Remote Sensing of Environment*, Vol. 79, No. 1, pp. 1-14.

Tatem, A.J., Lewis, H.G., Atkinson, P.M. & Nixon, M.S., 2003. Increasing the spatial resolution of agricultural land cover maps using a Hopfield neural network. *International Journal of Geographical Information Science*, Vol. 17, No. 7, pp. 647-672.

ACKNOWLEDGEMENTS

This work was supported in part by Open Research Fund from State Key Laboratory of Geological Processes and Mineral Resources (GPMR05-03), China University of Geosciences, the National Natural Science Foundation of China (Grant No.40201033) and Innovation Grant of Chinese Academy of Sciences (V36400).